

JUN 02 1995 35

ENGINEERING DATA TRANSMITTAL

1. EDT 158991

Sta. 21

2. To: (Receiving Organization) Distribution		3. From: (Originating Organization) Risk Assessment/D46EA		4. Related EDT No.: 605978	
5. Proj./Prog./Dept./Div.: 102AP TANK/WM/200A		6. Cog. Engr.: R. F. Jimenez		7. Purchase Order No.: N/A	
8. Originator Remarks: To examine the probability of and the damage potential resulting from dropping a mixing pump in Tank 102 AP				9. Equip./Component No.: N/A	
11. Receiver Remarks:				10. System/Bldg./Facility: 102 AP Tank/200A/WM	
				12. Major Assm. Dwg. No.: N/A	
				13. Permit/Permit Application No.: N/A	
				14. Required Response Date: 05/23/95	

15. DATA TRANSMITTED					(F)	(G)	(H)	(I)
(A) Item No.	(B) Document/Drawing No.	(C) Sheet No.	(D) Rev. No.	(E) Title or Description of Data Transmitted	Approval Designator	Reason for Transmittal	Originator Disposition	Receiver Disposition
1	WHC-SD-WM-ER-436	A11	0	Dropping of Mixing Pump in Tank 102 AP	S	1	1	

16. KEY		
Approval Designator (F)	Reason for Transmittal (G)	Disposition (H) & (I)
E, S, Q, D or N/A (see WHC-CM-3-5, Sec.12.7)	1. Approval 2. Release 3. Information 4. Review 5. Post-Review 6. Dist. (Receipt Acknow. Required)	1. Approved 2. Approved w/comment 3. Disapproved w/comment 4. Reviewed no/comment 5. Reviewed w/comment 6. Receipt acknowledged

(G)	(H)	17. SIGNATURE/DISTRIBUTION (See Approval Designator for required signatures)				(G)	(H)
Reason	Disp.	(J) Name	(K) Signature	(L) Date	(M) MSIN	Reason	Disp.
1	1	Cog. Eng. R. F. Jimenez	(5) <i>R.F.J.</i>	5/26-95	S4-43	3	
1	1	Cog. Mgr. G. N. Hanson	<i>G.N.H.</i>	5/24/95	S5-01	3	
1	1	QA M. Bhangoo	<i>M. Bhangoo</i>	5/19/95	S1-57	3	
1	1	Safety S. E. Hulsey	<i>S.E.H.</i>	5/13/95	S3-08	3	
3		C. F. Hoffman	<i>C.F.H.</i>	5/13/95	S4-43	3	

18. <i>HH-64</i> J.E. Kelly Signature of EDT Originator <i>J.E. Kelly</i> 5/19/95 Date		19. Rafael F. Jimenez Authorized Representative for Receiving Organization <i>Rafael F. Jimenez</i> 5/26/95 Date		20. G. N. Hanson Cog. Manager <i>G.N.H.</i> 5/20/95 Date		21. DOE APPROVAL (if required) Ctrl. No. <input type="checkbox"/> Approved <input type="checkbox"/> Approved w/comments <input type="checkbox"/> Disapproved w/comments	
--	--	---	--	---	--	---	--

DISCLAIMER

Portions of this document may be illegible in electronic image products. Images are produced from the best available original document.

RELEASE AUTHORIZATION

Document Number: WHC-SD-WM-ER-436, Rev. 0

Document Title: Dropping of Mixing Pump in Tank 102-AP

Release Date: 6/2/95

**This document was reviewed following the
procedures described in WHC-CM-3-4 and is:**

APPROVED FOR PUBLIC RELEASE

WHC Information Release Administration Specialist:

V. L. Birkland

V.L. Birkland

6/2/95

TRADEMARK DISCLAIMER. Reference herein to any specific commercial product, process, or service by trade name, trademark, manufacturer, or otherwise, does not necessarily constitute or imply its endorsement, recommendation, or favoring by the United States Government or any agency thereof or its contractors or subcontractors.

This report has been reproduced from the best available copy. Available in paper copy and microfiche. Printed in the United States of America. Available to the U.S. Department of Energy and its contractors from:

U.S. Department of Energy
Office of Scientific and Technical Information (OSTI)
P.O. Box 62
Oak Ridge, TN 37831
Telephone: (615) 576-8401

Available to the public from:

U.S. Department of Commerce
National Technical Information Service (NTIS)
5285 Port Royal Road
Springfield, VA 22161
Telephone: (703) 487-4650

SUPPORTING DOCUMENT

1. Total Pages **59**

2. Title

DROPPING OF MIXING PUMP IN TANK 102-AP

3. Number

WHC-SD-WM-ER-436

4. Rev No.

0

5. Key Words

**Dropping Mixing Pump in Tank 102-AP
EDT 158991**

6. Author

Name: **R. F. Jimenez**

R. F. Jimenez
Signature

7730/
Organization/Charge Code **D46EA**

7. Abstract

The ultimate goal of the study is to assess the need for installation of an impact limiter before pulling the AP-102 mixer pump.

8. **RELEASE STAMP**

**OFFICIAL RELEASE
BY WHC
DATE JUN 02 1995**

35

Sta. 21

CONTENTS

1.0 BACKGROUND 1-1
1.1 PURPOSE OF STUDY 1-1
1.2 SYSTEM GEOMETRY AND PUMP IMPACT 1-1

2.0 RESULTS AND CONCLUSIONS 2-1
2.1 PUMP IMPACT EFFECTS 2-1
2.2 THE IMPACT LIMITER 2-2

3.0 CALCULATIONS OF PUMP AND TANK BOTTOM INTERACTIONS 3-1
3.1 PUMP IMPACT VELOCITY 3-1
3.2 TANK BOTTOM PERFORATION PROBABILITY 3-4
 3.2.1 Perforation Calculations for Steel Liners 3-4
 3.2.2 Concrete Penetration 3-5
3.3 STRAIN ENERGY ANALYSIS 3-7

4.0 FREQUENCY OF PUMP DROP 4-1

5.0 PERSONNEL EXPOSURE DURING INSTALLATION OF IMPACT LIMITER 5-1

6.0 REFERENCES 6-1

APPENDIXES

A A-1
B DETAILS OF MISSILE STRIKE AND PENETRATION CALCULATIONS B-1

LIST OF FIGURES

1-1	Sections from Braun Hanford Co. Drawing H-2-90534 "Tank Cross Section, 241-AP Tanks"	1-2
1-2	Sections from Braun Hanford Company Drawing H-2-90534 "Tank Cross Section, 241-AP-Tanks"	1-3
3-1	Height Dependent Velocity for Dropped Pump Assembly	3-2
3-2	Bottom Impact Velocity Versus Drop Height	3-3

LIST OF TABLES

3-1	Summary of Steel Liner Perforation Capability	3-5
3-2	Energy Absorption with 30 Ksi Compressive Steel Yield	3-8
3-3	Energy Absorption with 60 Ksi Compressive Steel Yield	3-8

ACRONYMS

BRL	Ballistic Research Laboratory
CEA-EDF	Commissariat a l'Energie Atomique - Electricité de France
DOE	U.S. Department of Energy
EPRI	Electric Power Research Institute, Palo Alto, CA
SAIC	Science Applications International Corporation
SRI	Stanford Research Institute
WHC	Westinghouse Hanford Company

This page intentionally left blank.

DROPPING OF MIXING PUMP IN TANK 102-AP**1.0 BACKGROUND****1.1 PURPOSE OF STUDY**

Dropping of the mixing pump in Tank 102-AP during its removal poses the risk of causing a leak in the tank bottom with attendant potential for public exposure from the leak. The purpose of this investigation is to examine the potential for causing such a leak (i.e., estimated frequency of leak occurrence); to qualitatively estimate leak magnitude if it is a credible event; and, finally to compare the worker hazard, in the installation of an impact limiter (should it be required), to that which the public might incur if a leak is manifest in the tank bottom. The ultimate goal of the study is, of course, to assess the need for installation of an impact limiter.

It should be noted that this tank is not a "Watch List" tank, so that immediate replacement of a disabled mixing pump is not required.

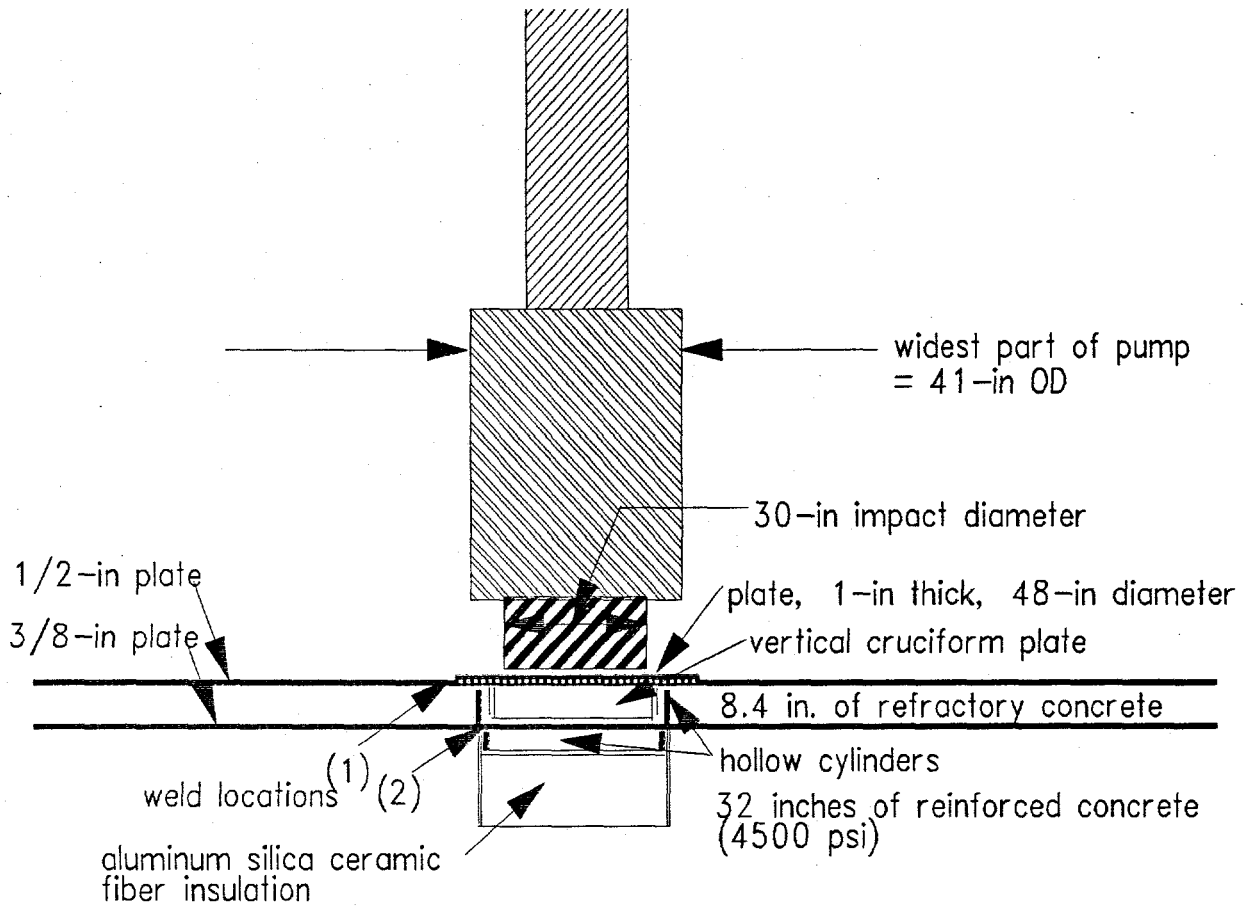
1.2 SYSTEM GEOMETRY AND PUMP IMPACT

Figure 1-1 is a schematic of the configuration of the pump and the tank bottom. The pump is shown in outline form, only, but the tank bottom is as close a representation of the actual tank bottom as can be inferred from detail 12 of the Braun Hanford Drawing of Ref. 2. A reproduction of detail 12 is included as Figure 1-2. The pump outline has been inferred from the Braun drawings of Refs. 2 and 3. The cavity below the pump in the center of the tank is an air distributor chamber. It extends both above and below the outer bottom tank wall with a hollow cylinder in each location. Each cylinder is welded to the outer plate. The upper hollow cylinder is open at the top and extends to 1/4-in below the inner (upper) tank plate. The bottom one is enclosed with a 1/2-in thick plate welded on its bottom and by being welded at its top to the bottom (outer) steel tank wall. Below the bottom hollow cylinder is a cylinder of alumina silica ceramic fiber insulation enclosed on the top and sides by 1/8-in thick plates. The total depth of the cavity scales to approximately 1-ft below the lower plate and the reinforced concrete is 32 inches in depth, so that 20 in of reinforced concrete are below the bottom of the air distributor cavity.

DISCLAIMER

This report was prepared as an account of work sponsored by an agency of the United States Government. Neither the United States Government nor any agency thereof, nor any of their employees, makes any warranty, express or implied, or assumes any legal liability or responsibility for the accuracy, completeness, or usefulness of any information, apparatus, product, or process disclosed, or represents that its use would not infringe privately owned rights. Reference herein to any specific commercial product, process, or service by trade name, trademark, manufacturer, or otherwise does not necessarily constitute or imply its endorsement, recommendation, or favoring by the United States Government or any agency thereof. The views and opinions of authors expressed herein do not necessarily state or reflect those of the United States Government or any agency thereof.

Figure 1-1. Sections from Braun Hanford Co. Drawing H-2-90534
"Tank Cross Section, 241-AP Tanks."



The nominal leak boundaries for the tank are the inner and outer tank liners. In order to induce a leak, both the inner and outer tank liners must be ruptured and leak paths through both the refractory concrete between the tank walls and the reinforced concrete below the outer (bottom) wall must be present. However, if the concrete base were not ruptured there would still be ample time to pump out the tank. The inner wall is 1/2-in thick except for the central 48-in diameter portion which is 1-in thick. The bottom wall is 3/8-in thick. The transition between the 1/2-in and 1-in portions of the inner tank bottom is a smooth taper as shown in Figure 1-2 (not stepped as shown in Figure 1-1).

It is also noted that recent measurements at three locations show that there is a 6-in layer of sludge at the tank bottom (17). This much sludge will significantly cushion the pump impact and reduce the likelihood of tank rupture, but it is not included in this analysis as an additional factor of conservatism.

2.0 RESULTS AND CONCLUSIONS

2.1 PUMP IMPACT EFFECTS

As shown in the subsequent sections, the physical design of the tank bottom makes it virtually impossible to engender a leak to the environment from a pump drop in Tank 102-AP. The frequency of drop, considering that the operation is treated as a "critical" operation (see Section 3), is approximately and conservatively estimated at $3E-05$ /operation.

In Section 3, it is shown that the inner tank bottom, acting by itself (i.e., if it were the only barrier present); the outer tank bottom, acting by itself; and the concrete base acting by itself will not be penetrated (or perforated) by a drop from this maximum possible height. The three acting together along with the refractory concrete augmenting the resistance, plus the resistance offered by the six inches of sludge on the tank bottom, make it inconceivable that the composite barrier (inner and outer tank wall, refractory concrete and reinforced concrete) could all be perforated. The only conceivable failure mechanism is cracking of the welds by impact. The weld between the two thicknesses of the inner tank plus one of the welds of the upper cylinder to the bottom tank wall would have to crack simultaneously and there would still have to be a leak path through both the types of concrete. Such a combination is considered virtually impossible, and if it were to occur, the leak rate would be extremely small. In Section 3.2.3, the potential for cracking the bottom concrete slab along with the welds is examined as part of a strain energy analysis.

If it were determined, following an accidental drop of the pump during its removal, that the tank were leaking, it could be emptied in roughly 170 hours (i.e., one week) (4). There is an operable transfer pump installed.

The relations used to determine steel and concrete perforation are primarily empirical and intended for use with a single homogeneous material. These are applied, in this study, to a portions of a composite barrier, and while the different empiricisms all show no perforation, their predictions are significantly different. Furthermore, it is impossible to assert without question that the welds in the two steel tank walls will not crack. Therefore, a strain energy analysis has been performed, which shows which portions of the tank bottom are damaged by the impact and it includes a bounding estimate of the maximum damage which could be engendered in the bottom tank and reinforced concrete under the assumption that the inner tank and outer tank both rupture by brittle weld fracture without diminishing the energy of the falling pump. The maximum damage under these circumstances causes only local effects, and does not produce a leak path through the full 32-in concrete base mat.

The strain energy analysis shows that the leak-protecting barriers of the tank, the inner and outer tank wall and the bottom concrete base mat very readily absorb the impact energy without failing, which verifies the conclusions reached with the empirical penetration algorithms.

Therefore, four separate analyses have led to the following conclusions:

1. The inner bottom steel tank wall has sufficient strength acting by itself to prevent its perforation by the falling pump;
2. The outer bottom steel tank wall has sufficient strength acting by itself to prevent its perforation by the falling pump;
3. The 32-in slab of reinforced concrete below the outer bottom tank wall has sufficient strength acting by itself to prevent its perforation by the falling pump;
4. A strain energy analysis has shown that the components can absorb the energy of the pump without compromise of leak protecting boundaries.

Furthermore, it is not credible that a crack could be engendered in the bottom concrete slab which would allow it to provide a path to the environment from a leak through cracked welds in the steel tank walls.

2.2 THE IMPACT LIMITER

An exposure of between 5 and 10 person-rem has been estimated for installation of the impact limiter and would be distributed among several workers. In view of the determination that a leak having any radiological impact would not be manifest and additionally that operational experience has shown that it is not necessary in terms of safety to have a mixer pump in operation. The results of this study indicate that the installation of the limiter has a negative impact both on cost and on safety.

3.0 CALCULATIONS OF PUMP AND TANK BOTTOM INTERACTIONS

3.1 PUMP IMPACT VELOCITY

The pump velocity at impact determines perforation capability of the tank bottom. In air, the air resistance can be neglected for the pump (12,000 lbs) and the velocity is determined by the classical equation for free fall:

$$V = (2gh)^{0.5}$$

In the liquid mixture, the pump's fall is impeded by the fluid resistance expressed by the following relation which can be found in any text on classical fluid mechanics:

$$F_f = A \rho V^2 C_d / 2$$

where

- F_f = force on the body due to fluid resistance (lbs),
- A = area of body perpendicular to direction of motion,
- ρ = density of the resisting fluid (slugs per ft³),
- V = velocity (fps) (of the dropping pump), and
- C_d = drag coefficient (unitless).

For high Reynolds numbers (> 100,000, which applies in this case), C_d is 1.

The terminal velocity of the body in the fluid is determined by equating F_f to the weight of the pump. Height dependent velocity is determined by differencing the acceleration due to gravity and that due to fluid friction and integrating numerically (since the resulting acceleration is non-uniform). Acceleration due to fluid friction is simply F_f/m , where m is the mass of the pump. Details of these calculations are contained in Appendix A-1. Results are shown in Figures 3-1 and 3-2.

Terminal velocity of the pump in the mixture (whose specific gravity is 1.2 from Ref. 5) is slightly less than 35 fps, and 35 fps is used in the analysis for convenience as well as conservatism. From Figure 3-1, it is seen that the pump exceeds fluid terminal velocity slightly at the 31-ft fluid surface when dropped from the top (50 ft) and slows to terminal velocity by the time it reaches the tank bottom. When dropped from the fluid surface it accelerates from 0 to near terminal velocity by the time it reaches the tank bottom.

Figure 3-2 shows bottom impact velocity as a function of drop height for two densities of the fluid. The 1.0 specific gravity covers the case where the suspended solids have settled out. This may be true if the mixing pump has been disabled for some time. Note that the impact velocity difference is only 3 fps for the maximum drop height, which is not very significant. Furthermore, if the solids have settled out, the sludge on the bottom affords a good impact cushion. Therefore, a 35 fps velocity impact on the bare (no sludge) tank bottom is considered a conservative scenario.

Figure 3-1. Height Dependent Velocity for Dropped Pump Assembly.

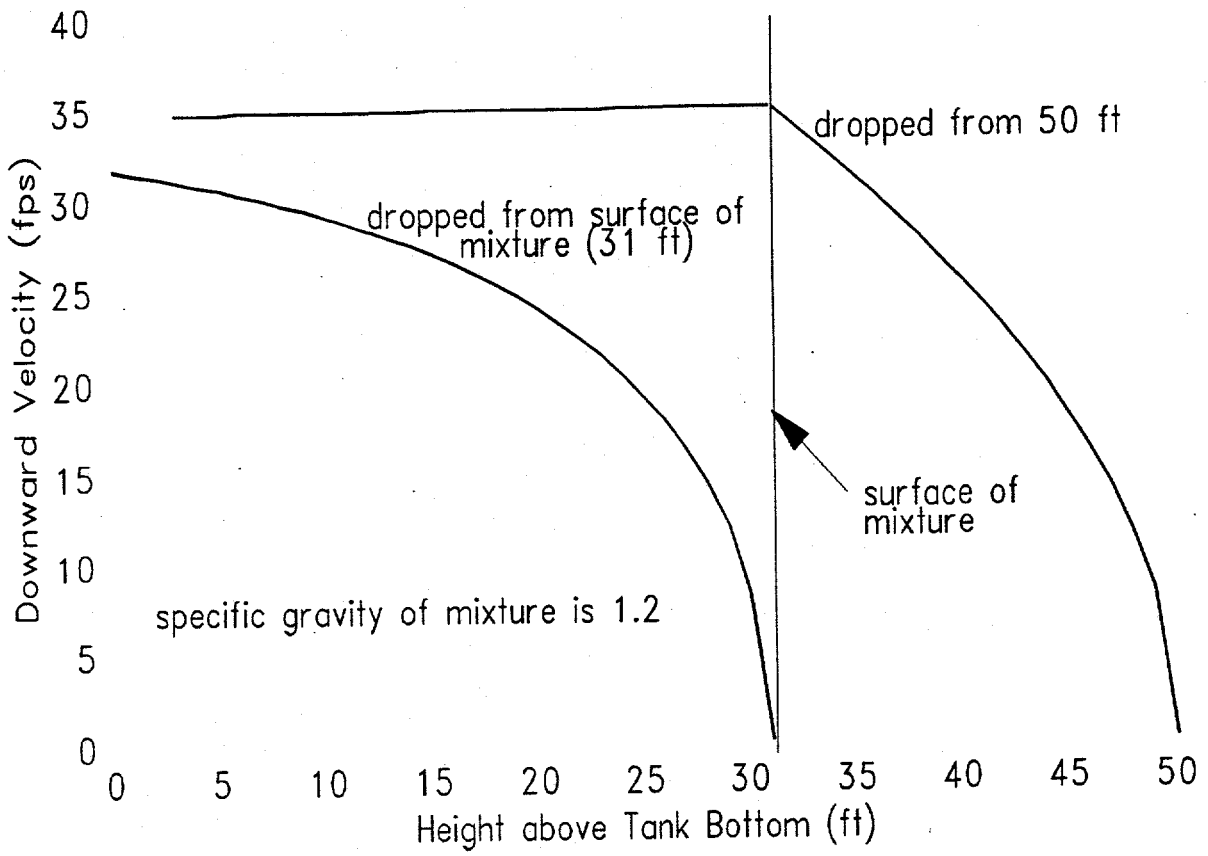
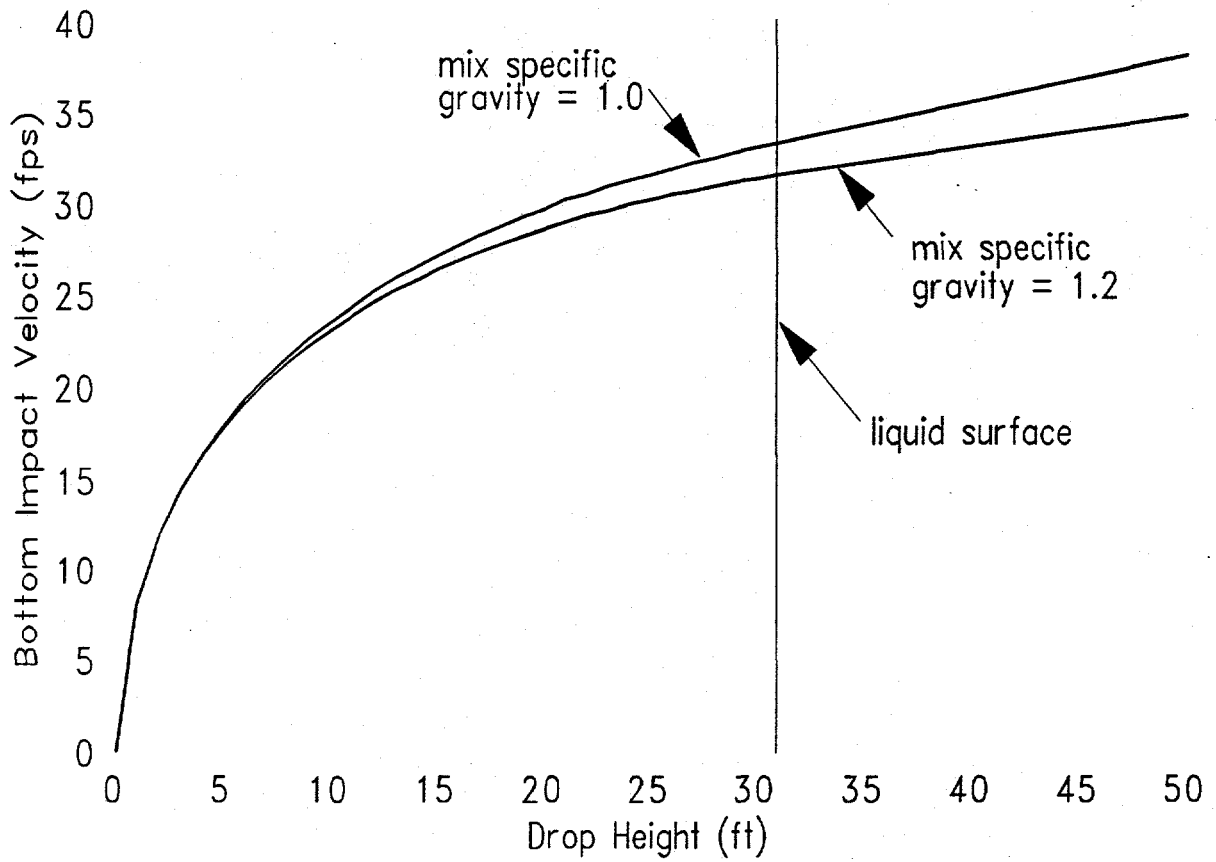


Figure 3-2. Bottom Impact Velocity Versus Drop Height.



3.2 TANK BOTTOM PERFORATION PROBABILITY

Exact calculation of the interaction of the pump with the tank bottom, particularly considering the complex geometry of the bottom center, is very difficult. An accurate estimate would require the use of a finite element code with plastic response modelling capability. Even with such sophistication, the Westinghouse Hanford Company (WHC) structural organization considers that such a prediction would be questionable (6). However, a bounding prediction (one whose conservatism is not questioned) can be made. This is done by four calculations: (1) determination of perforation capability of the inner steel liner by itself; (2) determination of the perforation capability of the outer steel liner by itself; (3) determination of concrete penetration by itself (this is the 4500 psi reinforced concrete as indicated by Reference 1); and (4) a strain energy determination of the effects of the pump impact on the tank bottom components including the damage to the reinforced concrete if the inner steel tank plate bottom provides no protection.

3.2.1 Perforation Calculations for Steel Liners

The integrity of the inner steel liner has to be compromised for any leak to take place. This liner is 1-in thick for its first 24-in radius from the center and then slopes to a thickness of one-half in beyond that point. It is supported on the bottom by refractory concrete (see Figures 1-1 and 1-2). However, since the refractory concrete compressive strength is small, only 130 psi (6), its presence is ignored, which is conservative. Two potential failure mechanisms are considered. One is failure at a 30-in diameter corresponding to the lower, smaller end of the pump shown in Figure 1-1 penetrating through the 1-in thick portion of the liner. The other is failure at the 48-in diameter interface between the 1-in and the 1/2-in portions and failure is considered to take place in the 1/2-in plate. In the latter case, the 1-in plate is treated as a rigid body and part of the pump missile. This treatment is conservative because it ignores the energy deposited in shear, compression and tension (the latter from stretching in its plane as membrane stress as it is elongated by deflection) in the 1-in-thick plate. The bottom 3/8-in plate is calculated simply as homogenous constant-thickness plate (which it is).

Three different perforation algorithms are used: (1) the Hagg-Sankey method which is recommended by the Electric Power Research Institute (Refs. 7,8); (2) the Ballistic Research Laboratory (BRL) formula which is recommended by U.S. Department of Energy (DOE) (9,10); and (3) the Stanford Research Institute (SRI) formula (11) which, although not specifically recommended by the Electric Power Research Institute, Palo Alto, CA (EPRI) or DOE has been recognized for decades as a reasonable estimator. Formula descriptions and calculational details are in Appendix A. Results are shown below in Table 3-1. The algorithms calculate the pump impact velocity which would be required to perforate the plate. For added perspective, the results of Table 3-1 include the ratio of energy available in the missile to the energy required to perforate. The Hagg-Sankey and the SRI formulas are tuneable within limits because of choice of parameters (discussed more fully in the Appendices). Parameters are chosen conservatively for both these methods and they are chosen deliberately to give more conservative results than the BRL formula.

Table 3-1. Summary of Steel Liner Perforation Capability.

Failure Mode	Algorithm	Perforation Velocity (fps)	Energy Ratio*
Inner Plate			
Fails through 1-in plate at 30-in diameter	Hagg-Sankey ^a	83	0.18
	SRI	111	0.1
	BRL [#]	124	0.08
Fails through 1/2-in plate at 48-in diameter	Hagg-Sankey ^a	77	0.2
	SRI	79	0.17
	BRL [#]	104	0.11
Outer Plate			
Fails through 3/8-in plate at 30-in pump diameter	Hagg-Sankey ^a	46	0.6
	SRI	59	0.35
	BRL [#]	59	0.35

Ratio of available missile energy to that required for perforation

^a Method recommended by Electric Power Research Institute

[#] Method recommended by U.S. Department of Energy

There are significant differences in the values predicted by the different algorithms but all predict that neither tank liner will fail. There is very little difference in energy required for engendering the two different postulated potential failure modes in the inner liner. It is difficult to determine which one would actually operate if the velocity were high enough for failure. As indicated above, the second method (failure through the 1/2-in section) ignores some energy dissipation mechanisms. As long as neither comes close to predicting failure, it doesn't matter which is more likely.

3.2.2 Concrete Penetration

The bounding estimate for concrete penetration, only, is to assume that the minimum concrete area available to resist penetration is that between the 41-in maximum pump diameter and the 36-in diameter air distributor cavity and consider that area is maintained throughout the 32-in thickness. This is a

conservative assumption since at the 12-in depth corresponding to the bottom of the air distributor cavity, the area of the cavity is added to the resisting concrete. The area used is:

$$\pi/4(41^2 - 36^2) = 302.4 \text{ in}^2$$

The penetration algorithms used are based on a circular cross-section missile, so that the diameter D is defined as:

$$2(A/\pi)^{.5}$$

where A is the projected impact area.

The two formulas used to determine the limiting case of concrete penetration are the Commissariat a l'Energie Atomique - Electricité de France (CEA-EDF) formula (named for the French equivalent of our Nuclear Regulatory Commission and the main French Electrical Utility Company who co-developed the algorithm - Ref. 12) and the BRL formula for concrete (11).

The CEA-EDF concrete penetration formula is:

$$= 0.765\sigma_c^{-.375}(W/D)^{0.5}V^{0.75} T$$

Where

- T = barrier thickness in inches;
- σ_c = concrete compressive strength in psi;
- W = missile weight in pounds;
- D = effective diameter in inches;
- V = incident velocity normal to barrier in fps.

Written in terms of required velocity for perforation of thickness, T, the relation is:

$$V = 1.43 T^{1.33} \sigma_c^{0.5} (D/W)^{0.667}$$

The BRL formula is:

$$T = 427\sigma_c^{-.5}WD^{-1.8}(V/1000)^{1.33}$$

or, in terms of velocity:

$$V = 10.65 T^{0.75}\sigma_c^{0.375}W^{-0.75}D^{1.35}$$

The CEA-EDF formula has been recommended by EPRI. DOE has not yet published its document recommending algorithms for concrete penetration (9), but its author has indicated that the BRL formula will be recommended (10) when it is published. The CEA-EDF formula predicts a perforation velocity of 134 fps for 32 inches of concrete at such an impact area and the BRL prediction is 163 fps.

If we were to assume that the missile (i.e., the dropping pump) could stay within the air distributor cavity for a sufficient depth to impact the cavity bottom unimpeded and with the 30-in bottom pump diameter impacting the surface, then the thickness of concrete which resists penetration would be 20 inches. In such a hypothetical impact, the CEA-EDF formula would predict a

95 fps perforation velocity and the BRL would predict one of 203 fps. Obviously, the integrity of the bottom concrete is not even remotely threatened by the dropping of the pump.

3.3 STRAIN ENERGY ANALYSIS

Because all the penetration formulas are empirical, and while they all conservatively show no penetration (or perforation), the fact that they are empirical and that they do differ has prompted a strain energy analysis of the reacting components at the tank bottom to assess the component damage from the falling pump. The results are shown in Tables 3-2 and 3-3. The details of the analysis, including needed derivations, are in Appendix A-3.

The major energy absorbing mechanisms are the cylinder between the two tank bottom liners, the cruciform plate also between the liners and the refractory (insulating) concrete between these liners. Two different compressive yield strengths (30 Ksi and 60 Ksi) were assumed to bracket the effects, because the response is highly dependent on this yield strength and this range was felt to cover the possibilities for the steel compression members (the cylinder wall and the cruciform plate). With the high-strength (60-psi) steel, enough of the energy is transferred to the concrete base mat that it becomes a significant energy absorber.

It is observed that the primary leak protection boundaries, the inner steel liner and especially the outer steel liner and the concrete base mat are not significantly impacted by the pump drop. This corroborates the conclusion drawn from the empirical penetration algorithms, that engendering a significant leak is not a credible event. The vertical steel members and the refractory concrete between the two liners are an effective shock absorber for the primary leak-protecting boundaries.

The differences between the 30 psi and the 60 psi cases (Tables 3-2 and 3-3) are discussed in Appendix A.3. In Appendix A.3, a worst case situation with the strain energy is analyzed. It is based on the assumption that all welds in both tank liners fail with no loss of impacting energy. In this case the cylinder between the tank liners is forced onto the concrete at the edge of air distributor cavity. While it chips off a region of concrete on the side of the air distributor cavity, it is demonstrated in A.3 that this does not compromise the leak integrity of the concrete base mat.

Table 3-2. Energy Absorption with 30 Ksi Compressive Steel Yield.

Component	Disp/Defl (in)	Elastic Energy	Plastic Energy	Total Energy	Per Cent
Upper Shell	1.29/1.29	4.9 E04 in-lb	0	4.9E04	1.85
Refractory Concrete	1.29/1.25	neg.	2.48 E05	2.48 E05	9.34
Cylinder Wall	1.043/1.0	7271	1.7 E06	1.71 E06	64.1
Cruciform Plate	1.29/0.625	4467	6.14E 05	6.18 E05	23.3
Lower Shell	0.043	12	0	12	neg
Concrete Base Mat	0.043	36173	0	36173	1.36
Total	1.29	9.7 E04	2.56 E06	2.66 E06	100

Table 3-3. Energy Absorption with 60 Ksi Compressive Steel Yield.

Component	Disp/Defl (in)	Elastic Energy	Plastic Energy	Total Energy	Per Cent
Upper Shell	.829/.829	2.61 E04 in-lb	0	2.61E 04	0.98
Refractory Concrete	.829/.625 (av)	neg.	1.25 E05	1.25 E05	4.7
Cylinder Wall	0.79/0.375	2.9 E04	1.27 E06	1.3 E06	49
Cruciform Plate	0.625/neg.	1.8 E04	0	1.8 E04	0.67
Lower Shell	0.204	1318	0	1318	0.05
Concrete Base Mat	0.204	1.66 E05	1.03E06	1.2E6	45
Total	0.829	2.4 E05	2.37 E06	2.67 E06	100

Displacement and deflection: total movement of top surface, and movement relative to bottom surface, respectively.

4.0 FREQUENCY OF PUMP DROP

Since the pump is to be removed via crane, data on crane failures which caused dropping of the load are appropriate. A problem with the data sources found for crane drops is that most of it has been reported as drop rate per hour of operation of a given facility instead of probability per crane operation. It has been difficult to construct a robust data base on a per operation basis. The best source appears to be that from the Portsmouth, Ohio, UF₆ operations (13) which, since it involves operations with radioactive substances, would likely be from operations which match the level of caution employed in removing tank pumps. From Reference 13 crane event frequencies which can potentially cause a load drop are summed to produce a final estimate. Such an summation is conservative, since these are only potential, and not actual load drops. These are:

Lifting lug failures:	7.5 E-06 per operation
Uncontrolled Bridge or Trolley Movement:	4.6 E-06 per operation
Cable Failure:	8.4 E-05 per operation
Hoist Brake Failure:	1.0 E-03 per operation
Total:	1.1E-03 per operation

The data from Reference 13 indicates the hoist brake failure rate was deliberately chosen very conservatively. None of the failures caused anything more than load drift, not a catastrophic drop. For the type of drop concerned in this case, it would seem reasonable to remove this failure from the data. Also for the crane that will be used in this pump removal there is no bridge or trolley, so this failure should also be removed. The cable failures generally did not result in load drop. Portsmouth data, then, would indicate, still conservatively, a drop rate of approximately 7.5E-06 per operation.

Los Alamos National Laboratory reported a mean frequency of 3.85E-05 per operation for dropping the mixing pump being inserted in Tank 101-SY. They based their analysis on NUREG 0612, Control of Heavy Loads at Nuclear Power Plants. NUREG-0612 was an analysis of cranes used to remove the head off a pressure vessel or spent fuel in a power plant. NUREG-0612 used naval data for crane failure and found it to be 2.0E-05 per operation. It was not clear whether all the failure modes could cause a load drop. The naval data used indicated that there were 43 failures in the data base from February, 1974 to October, 1977. Seven of these were component failures. The remaining 36 were human errors; one was in design, two were in maintenance, eleven were distractions, eight were due to training, eleven due to not following procedures, and three were rigger errors. Hanford is required to follow DOE-RL 92-36, *Hanford Site Hoisting and Rigging Manual*. This should help eliminate some of the potential human errors.

From these data sources, it can be inferred that a rate of 3E-05 per operation is a reasonable and a conservative number.

This page intentionally left blank.

5.0 PERSONNEL EXPOSURE DURING INSTALLATION OF IMPACT LIMITER

While there appears to be no justification for installation of an impact limiter based on the analysis presented herein, and assessment of the approximate personnel dose resulting from such an installation has been made. WHC personnel have supplied estimated man-hours at various locations where workers would have to be in order to install an impact limiter, and dose levels at these locations have been measured. From these, an estimated upper limit person-rem value of 10 and an expected mean value of 5 has been estimated for this effort.

This page intentionally left blank.

6.0 REFERENCES

- BC-TOP-9-A, Rev. 2, 1974, Topical Report, "Design of Structures for Missile Impact," Bechtel Power Corporation, San Francisco, California, September, 1974.
- Braun Hanford Drawing H-2-90534, *Tank Cross Section, 241-AP Tanks*.
- Barrett, Haentjens & Co. Preliminary Drawing, 1986, *Proposed Submersible Pump/Mixer*, April 28, 1986.
- Barrett, Haentjens & Co. Elevation Drawing, 1986, *Hazleton 10 GN SSB Pump/Mixer, Model # 447-150-1200(R)*, July 17, 1986, R232197, N20056.
- DPST-88-830, 1988, "Tornado and Wind Missile Hazards to TRU Waste Containers at the Savannah River Burial Ground", December 1988.
- Den Hartog, J. P., 1952, *Advanced Strength of Materials*, McGraw-Hill Book Company, New York, New York.
- EDT 607537, 1994, *Double Shell Tanks Emergency Pumping Plan*, Sept 23, 1994.
- Hagg, A. G. and G.O. Sankey, 1974, "The Containment of Disc Burst Fragments by Cylindrical Shells" *Journal of Engineering for Power*, TRANS ASME, p. 114-123, April 1974.
- McDonald, J. R. "Tornado Missile Criteria for DOE Facilities", LLNL, Livermore, California, 1993 (yet to be published).
- Patton, E., et. al., 1981, "Probabilistic Analysis of Low Pressure Steam Turbine Generator Events," *Draft EPRI Report RP 1549-1*, Battelle Northwest Laboratories, Richland, Washington.
- Private communication, J. R. McDonald of Texas Tech. University to Bryce Johnson of Science Applications International Corporation (SAIC), June 1994.
- Private communication, John Strehlow, WHC, to Bryce Johnson, SAIC; October 1994.
- "Risk of UF₆ Handling Facilities, Appendix Y, Reliability Data", draft report for review, Portsmouth Ohio Diffusion Facility, 9/29/89.
- Seely, Fred B., 1949, *Resistance of Materials*, 3rd Ed., John Wiley & Sons, London, February, 1949.
- Sliter, G. E., 1980, "Assessment of Empirical Concrete Impact Formulae", *Journal of the Structural Division*, ASCE, Vol 106, NO. ST, May, 1980.
- Sludge depth measurement, 1995, "Communication with Rafe Jimenez of WHC with Bryce Johnson", March, 1995.
- WHC-SD-WM-TRP-168, Rev. 1, *Tank 241-AP-102 Characterization and Grout Produced Test Results*.

WHC-SD-WM-ER-436, Rev. 0

This page intentionally left blank.

Appendix A

This page intentionally left blank.

APPENDIX A

A1.0 MISSILE VELOCITY AT IMPACT

When the missile is dropped from the top of the tank (50 ft above the bottom), 19 ft of free fall are assumed from the top to the liquid surface, and the velocity at fluid impact is that from the classical equation of falling bodies in a vacuum (air resistance is considered negligible for a 6-ton pump assembly falling 19 ft).

$$V = (2gh)^{.5} = (64.4 \times 19)^{.5} = 34.98 \text{ fps}$$

The resistance to solid motion in a fluid is governed by the Stokes Equation,

$$F_r = A\rho V^2 C_d / 2,$$

where ρ is fluid density, V is velocity of the body and C_d is the dimensionless drag coefficient, which for bodies of this type and high Reynolds numbers ($> 100,000$, which applies for the dropping pump) is 1. Terminal velocity in the fluid is determined by the Stokes equation by setting F_r in the defining equation equal to the weight of the falling body (12,900 lbs in this case, when the pump is assumed to carry 75 gallons of waste). The solution for V is then:

$$V = [12,900 / 9.17 \times 2 \times 2.33]^{1/2}$$

The result is 34.82 fps (nearly identical to the velocity with which the pump strikes the fluid surface).

The height-dependent velocity in the fluid, from which the curves of Figures 3-1 and 3-2 were generated, is determined by step-wise numerical integration on a spread sheet with the net acceleration at each 1-ft increment determined as the difference between g and the Stokes equation above divided by the pump mass. The acceleration was considered constant for the 1-ft distance and a new velocity calculated as the old velocity + at , where t , the time to travel 1 ft, is determined by $1/V$ with the velocity that of the preceding step.

The spreadsheet which produced the bottom curve of Figure 3-1 is included as Table A-1. The missile velocity from the curve at a height of 0 is the impact velocity. A similar numerical integration determined the impact velocity for the drop from the top (50 ft) by the same process, but starting with a velocity of 34.98 fps instead of 0. The curves of Figure 3-2 were taken from Figure 3-1 by using the abscissa as the difference between 31 feet and the abscissa of Figure 3-1. A separate curve analogous to the bottom curve of Figure 3-1 was generated for the 1.0 density fluid.

**A2.0 CALCULATIONS OF PUMP PENETRATION VELOCITY
FOR INNER TANK BOTTOM**

The values of Table 3-1 were determined from the Hagg-Sankey, the Ballistic Research Laboratory (BRL) and the Stanford Research Institute (SRI) empirical penetration algorithms. The classical Bechtel publication, BC-TOP 9 of Reference 11 is recommended to the reader for a discussion of the BRL and SRI formulas. Appendix B contains a discussion of the Hagg-Sankey Formula. The BRL and SRI formulas are reproduced below. The Hagg-Sankey method does not contain a single formula, but is a rather complex process which allows a bi-modal failure mechanism (by shear and compression under certain circumstances, and by tension in the plane of the barrier under other circumstances). These are explained in Appendix B.

Table A-1. Numerical Integration for Pump Velocity in Fluid.

Drop Height	V ²	Up Acc.	Net Acc.	Delta Time	New V
31	0				0
30	0		32.2	0.249222	8.024961
29	64.4	1.709207	30.49079	0.124611	11.82446
28	139.8177	3.71083	28.48917	0.08457	14.2338
27	202.601	5.377128	26.82287	0.070255	16.11825
26	259.7979	6.895161	25.30484	0.062041	17.6882
25	312.8723	8.303781	23.89622	0.056535	19.03917
24	362.4899	9.620655	22.57934	0.052523	20.22511
23	409.055	10.85652	21.34348	0.049443	21.28041
22	452.8557	12.01901	20.18099	0.046992	22.22874
21	494.117	13.1141	19.0859	0.044987	23.08736
20	533.026	14.14677	18.05323	0.043314	23.86931
19	569.7439	15.12128	17.07872	0.041895	24.58482
18	604.4133	16.04142	16.15858	0.040676	25.24208
17	637.1625	16.9106	15.2894	0.039616	25.84779
16	668.1082	17.73191	14.46809	0.038688	26.40753
15	697.3577	18.50821	13.69179	0.037868	26.92601
14	725.0101	19.24211	12.95789	0.037139	27.40725
13	751.1574	19.93608	12.26392	0.036487	27.85472
12	775.8855	20.59237	11.60763	0.035901	28.27144
11	799.2744	21.21313	10.98687	0.035371	28.66006
10	821.3992	21.80033	10.39967	0.034892	29.02293
9	842.3302	22.35585	9.844153	0.034456	29.36211
8	862.1336	22.88144	9.318563	0.034057	29.67948
7	880.8714	23.37875	8.821251	0.033693	29.97669
6	898.6022	23.84933	8.350666	0.033359	30.25527
5	915.3812	24.29465	7.905345	0.033052	30.51656
4	931.2601	24.71609	7.48391	0.032769	30.7618
3	946.2881	25.11494	7.085061	0.032508	30.99212
2	960.5113	25.49243	6.707571	0.032266	31.20854
1	973.9733	25.84972	6.350284	0.032043	31.41202
0	986.7152	26.18789	6.012106	0.031835	31.60342

The program written in the BASIC computer language which computes the values with these three formulas is reproduced in Table A-2.

The BRL formula is:

$$V = 1058.6 (TD)^{0.75}/W^{0.5}$$

where

- V = missile velocity required for perforation in fps;
- T = steel barrier thickness in inches;
- D = missile diameter in inches (for a non-circular section, D is calculated as $2(A/\pi)^{0.5}$ where A is cross-sectional area of the missile in inches);
- W = missile weight in pounds.

The SRI formula is:

$$V = (64.4 D F1/W)^{0.5}$$

where the terms are the same as defined for BRL, except that F1 is defined as:

$$50000(0.344 T + 0.00806 T_w T)$$

where T_w is the dimensions of the square "frame" surrounding the point of missile impact. The frame defines points of rigid support. For this application, this is really the diameter of the tank bottom, but for conservatism, 200 inches has been used (smaller frames predict smaller perforation velocities).

Table A-2. Program for Calculating Missile Penetration by Hagg-Sankey and Other Methods.

```

10 REM calculating missile/steel-wall impacts
12 REM INPUT MISSILE PARAMETERS
REM if q = 0 don't calculate other penetration algorithms
14 INPUT "other calcs ="; q
15 INPUT "MEAN MISSILE THICKNESS IN INCHES="; MT
24 INPUT "wall interaction parameter="; IP
26 INPUT "tensile range factor="; TR
30 INPUT "min missile area in sq inches="; FA
40 MP = 2 * (FA / MT + MT)
50 INPUT "missile weight in pounds"; WM
55 INPUT "missile length in inches="; LW
60 INPUT "steel wall thickness in inches"; TW
78 INPUT "normal velocity ="; VM
79 AM = FA
80 PH = IP / (1 - EXP(-.00138 * VM))
PRINT "PH ="; PH
85 A1 = AM + 1.36 * PH * TW * SQR(AM)
90 REM calculate m2
100 M2 = 8.809999E-03 * A1 * TW
110 EC = 292 * AM * TW
120 ES = 4500 * TW ^ 2 * SQR(AM)
130 M1 = WM / 32.2
140 E1 = .5 * M1 * VM ^ 2 * (1 - M1 / (M1 + M2))

```

Table A-2. Program for Calculating Missile Penetration
by Hagg-Sanke and Other Methods. (cont'd)

```

150 TE = EC + ES
155 Q1 = (M1 * VM / (M1 + M2)) ^ 2
160 IF E1 > TE THEN 220
165 PRINT
170 PRINT "wall does not fail in phase 1"
180 GOTO 400
220 M3 = 8.809999E-03 * AM * TW
230 M4 = M2 - M3
250 Q2 = 2 * TE * M4 - M1 * VM ^ 2 * (M4 - M1)
260 Q3 = (M1 + M2) * (M1 + M3)
266 RT = Q1 - Q2 / Q3
270 VE = SQR(Q1) - SQR(RT)
280 PRINT
282 PRINT "phase 1 penetration"
285 PRINT "phase 1 exit velocity="; VE
300 GOTO 600
400 E2 = .5 * M1 * VM ^ 2 * (M1 / (M1 + M2))
405 PRINT "Hagg-Sanke modified for thin metal:"
410 ET = 208 * (TR * MP * TW ^ 2 + AM * TW)
420 IF E2 > ET THEN 500
430 PRINT
435 PRINT "wall beach prevented"
440 GOTO 532
500 EV = SQR(Q1 - ET / (M1 + M2))
501 PRINT "q1="; Q1
502 PRINT "m1="; M1
503 PRINT "m2="; M2
510 PRINT
520 PRINT "wall fails in phase 2"
530 PRINT "phase 2 exit velocity="; EV
532 PRINT "shear and compression energy capacity="; TE
533 PRINT "tensile energy capacity="; ET
534 PRINT "missile energy for shear and compr.="; E1
535 PRINT "missile energy available for overcoming tension="; E2
536 PRINT "energy values are in ft-lbs"
540 PRINT "impact area in sq inches="; AM
545 PRINT "impact periphery in inches="; MP
550 PRINT "impact velocity in fps="; VM
551 PRINT "wall impact parameter="; IP
552 PRINT "tensile range indicator="; TR
555 PRINT "missile identifier="; ID
c3 = 0
c4 = 0
c5 = 0
c6 = 0
IF q = 0 THEN GOTO 1000
558 REM if c = 1, approximation adequate
559 REM if c = 0, try again
560 INPUT "c="; C
561 IF C > 0 THEN 600

```

Table A-2. Program for Calculating Missile Penetration by Hagg-Sankey and Other Methods. (cont'd)

```

578 INPUT "new am="; AM
580 MP = 2 * (AM / MT + MT)
590 GOTO 80
600 REM SRI formula
605 PRINT "if c3 = 0 don't calculate SRI velocity"
610 INPUT "c3="; c3
615 IF c3 = 0 THEN 670
620 INPUT "wall frame width in inches ="; WW
630 F1 = 50000! * (.344 * TW + .00806 * WW * TW)
635 PRINT "f1="; F1
640 D = 2 * (AM / 3.1415926#) ^ .5
645 PRINT "d="; D
650 VS = (64.4 * D * F1 / WM) ^ .5
660 PRINT "SRI perforation velocity ="; VS
670 PRINT "BRL Velocity"
680 PRINT "if c4 = 0, don't calculate BRL velocity"
690 INPUT "c4="; c4
700 IF c4 = 0 THEN 760
710 VB = 1058.565 * TW ^ .75 * D ^ .75 / WM ^ .5
720 PRINT "BRL perforation velocity = "; VB
760 T3 = (AM - FA) / (MT * LW)
940 AC = ATN(T3 / SQR(1 - T3 ^ 2)) * 57.29578
945 T4 = SQR(1 - T3) ^ 2
950 T5 = (AM - FA * T4) / (MT * LW)
952 AD = ATN(T5 / SQR(1 - T5 ^ 2)) * 57.29578
954 PRINT
956 PRINT "AC="; AC
958 PRINT "AD="; AD
960 P = AC / 90
962 P1 = AD / 90
965 PRINT "OTH ITERATE PEN. PROBABILITY="; P
970 PRINT "1ST ITERATE PEN. PROBABILITY="; P1
990 PRINT "tornado identifier="; TI
995 PRINT "missile identifier="; ID
1000 END

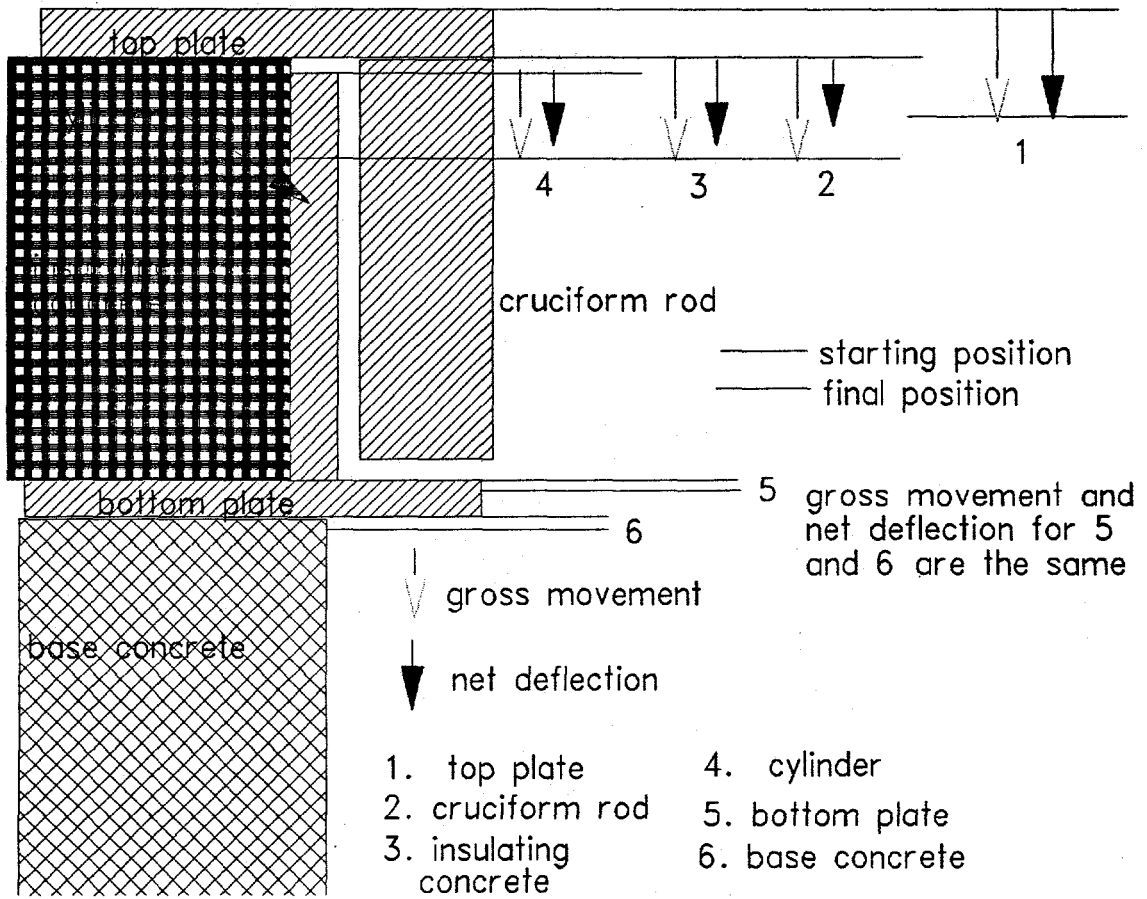
```

A3.0 STRAIN ENERGY ANALYSIS OF TANK BOTTOM RESPONSE TO DROPPED PUMP

A3.1 GENERAL CONSIDERATIONS

The kinetic energy of the dropped pump assembly as it hits the tank bottom has to be absorbed as strain energy in the various structural members at the tank bottom (as shown in Figures 1-1 and A-1). These include both the inner and the outer shell (upper and lower steel tank bottoms), the vertical cylinder attached (presumably welded) to the top of the outer (3/8-in) bottom plate and extending up to within 1/4-in of the bottom of the upper plate, the cruciform plate attached (presumably welded) to the bottom of the upper (1-in) bottom plate and extending down to within 5/8-in of, the refractory insulating

Figure A-1. Displacements and Deflections of Components at Bottom of Tank.



concrete and the base concrete below the lower bottom plate. The hollow cylinder below the lower bottom plate and the aluminum silica ceramic fiber insulation (these are not shown in Figure A-1) in the bottom of the air distributor chamber are not included among the energy absorbers both because significant displacement must occur in all the other components before these can react and because it is assumed that the fiber insulation can be displaced significantly without appreciable energy absorption. The lower hollow cylinder can be stressed only by stressing the fiber insulation.

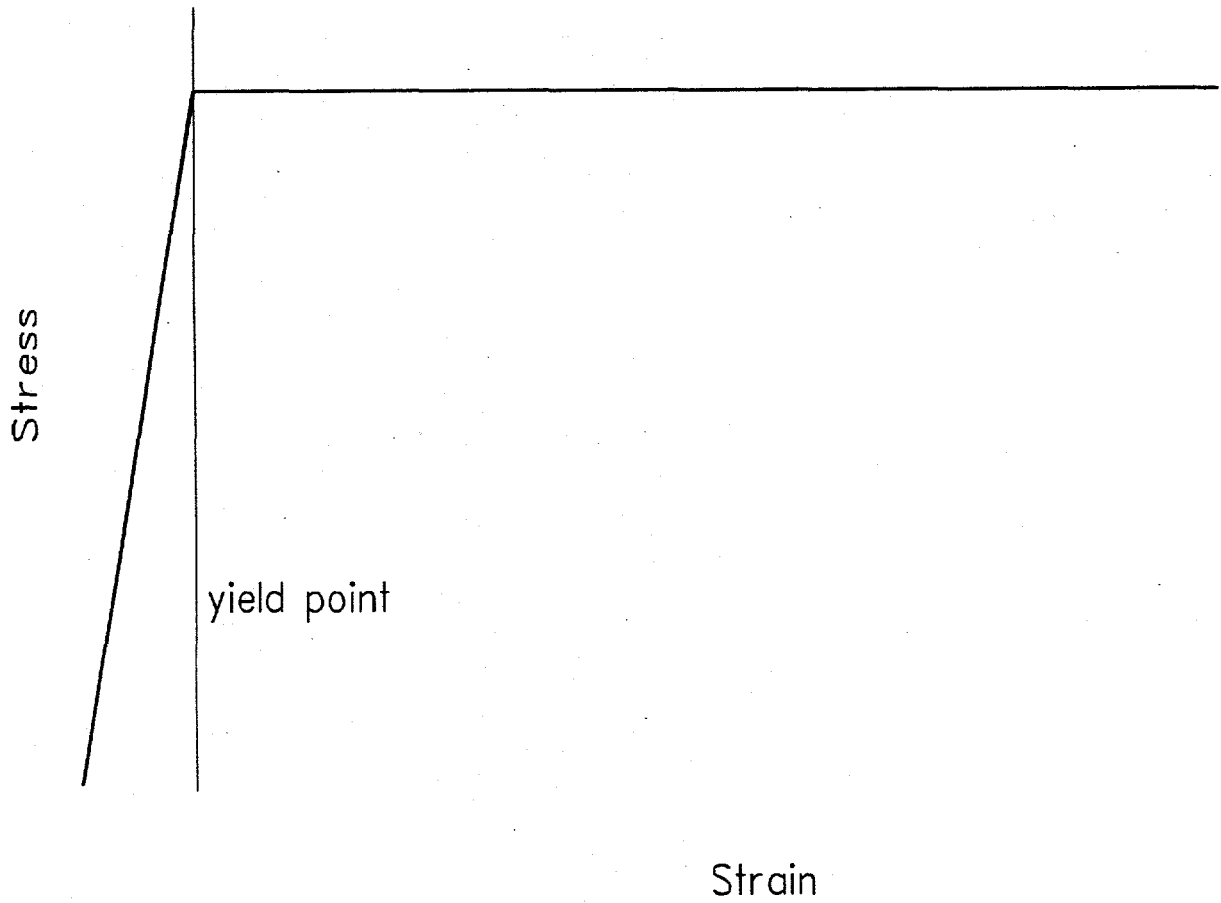
The absorption mechanisms are compression in the cylinder and the cruciform plate between the two tank shells, compression in both the refractory and base concrete and flexure in the two bottom tank shells. The compressive strength of the steel in the cylinder and the cruciform plate between the tanks shells is unknown and the radial extent of the effects of the impact in both the concrete and the bottom shells is not known. The unknown steel compressive strength is accommodated by evaluating over the full range of variation of this variable in steels (from 30,000 to 60,000 psi, see Ref.14, for example). The unknown radial extent is accommodated by evaluating what is considered a "reasonable-estimate" scenario and extending this to a bounding, obviously "worst-case" scenario, as well as investigating the general effects of this variation.

A3.2 ASSUMPTIONS

A precise allocation of the strain energy among these components would require the operation of a sophisticated finite element code and even that would be questioned (Ref. 6). However, the allocation can be approximated to the degree necessary for assessing tank integrity with reasonable assumptions regarding the displacements of the components. These assumptions include:

1. The two bottom plates deform as circular plates subject to a center load and are assumed to be fixed at their outer radii (that distance at which the impact effect ceases) (Equations 81 of Reference 16 define displacements and internal stress and moments for this case). Fixed at the outer radii simply means their slope in the radial direction is 0 at that point.
2. The two layers of concrete (refractory concrete between the bottom shells and the bottom base concrete) deform with the bottom plates and their displacement as a function of radius is governed by the displacement of the bottom steel plates.
3. The vertical steel cylinder and cruciform plate between the two bottom shells deform by pure compression, not by buckling.
4. The upper of the bottom plates is assumed to be 1/2-in thick throughout instead of having a 48-in diameter central portion which is 1-in thick.
5. The materials response model for compression in the steel and concrete is the so-called elastic-perfectly plastic model where the elastic response is governed by Hooke's law until yield and then yields indefinitely at the constant yield stress value thereafter (Figure A-2).

Figure A-2. Elastic, Perfectly Plastic Materials Response Model.



The first assumption is a reasonable one for the top plate because the refractory concrete on which it rests has only a 130 psi strength, so it is expected to have negligible effect on the plate deformation. On the bottom plate, however (since it is resting on 4500 psi concrete) there is an effect. An exact analytical solution would require an iteration between the central load on top and the radially dependent reaction load of the concrete from the bottom. The complexity of plate theory makes such an attempt untenable (i.e., much more work than using a finite element code). The approach is an artifice to define a radial displacement in the concrete for energy absorption calculations. The fixed-end assumption follows from the fact that a 0 slope is expected at the point where the shell reaction becomes negligible.

The justification for the second assumption follows from the fact that there is no reason to expect a separation between the steel and the concrete.

The third assumption is conservative relative to protection of the shells of the tank which prevent leakage. These vertical plates would be better energy absorbers if they did buckle. However, they are so well constrained and their vertical dimensions sufficiently short that the non-buckling assumption is not unreasonable.

The fourth assumption is conservative since it considers a reduced quantity of resisting steel. It is used because it reduces the complexity of the plate analysis.

The fifth assumption is a reasonable one for compression. Once yield occurs, the material has "no place to go" if it did rupture so it keeps on yielding.

While it is not an assumption, it should be noted that neither the cylinder wall nor the cruciform plate can punch through the bottom shell before either of them reach their yield stress (which, for compression, is the same as the ultimate stress). The fact that the empirical penetration algorithms showed no penetration of the bottom shell for missiles of lesser radii than that of the cylinder is 'a priori' evidence of this fact. However, it can be demonstrated by noting that at least one shearing surface augments the compression surface in the bottom plate. Since the compression area in the bottom plate equals that of the cylinder and the cruciform at the contact point, its resistance to punching is greater than the punching capability of the cylinder or cruciform. For the cruciform plate, both shear surfaces will resist perforation. Furthermore, in both cases stretching in the plane of the bottom plate (membrane stress) allows the tensile strength to augment shear and compression in resisting perforation.

A3.3 MATERIALS RESPONSE

A3.3.1 Compressive Response

Compression is modeled relatively easily. All strain energy is simply a product of force times displacement. In the elastic realm, force is proportional to displacement:

$$F = EA\varepsilon = Ead/L \quad (A-1)$$

where

- E = Young's Modulus, or modulus of elasticity (psi)
- A = cross sectional area of stressed body
- ε = strain (inches/inch)
- d = material displacement in direction of applied force
- L = dimension of body being stressed (in direction of force)

Work, or energy, denoted J, is the area under the plot of force versus displacement, which, with the Hooke's Law of proportionality, is a triangle whose area in terms of displacement and Young's Modulus is simply:

$$J = Ead^2/(2L) = F_{\max} d/(2) \quad (A-2)$$

In the plastic realm stress remains constant and work is simply $F_y d$, where F_y is the load on the body at yield.

A3.3.2 Strain Energy in the Bottom Tank Plates

The following equation represents the displacement in a circular plate clamped (fixed) at the outer radius and loaded with a central concentrated load. This is Equations 81 of Reference 16. This is a reasonable representation of the top plate load and an approximate one for the bottom plate load. This latter approximation improves when the cruciform plate engages the bottom plate.

$$w = \frac{PR^2}{16\pi D} \left[1 - \frac{r^2}{R^2} + 2 \frac{r^2}{R^2} \ln \frac{r}{R} \right] \quad (A-3)$$

In this relation w is displacement in inches at r (in inches), P is the central load in pounds, R is the maximum radius, D is the so-called plate stiffness defined by:

$$D = \frac{Et^3}{12(1-\mu^2)}; \quad (A-4)$$

where μ is Poisson's ratio, E is modulus of elasticity (psi) and t is plate thickness in inches. Using a $2.7E+07$ value for E, the respective values of D for 1-in, 1/2-in and 3/8-in plates are: $2.54E+06$, $6.35E+05$ and $1.34E+05$.

Three strain energy components are considered in the plate: radial bending, bending in the meridional plane (θ direction) and the energy of internal shear. Evaluating these internal components can be extremely arcane, but as long as the response remains elastic the total energy can be evaluated simply as $Pw/2$ where P is the eternally applied load and w is deflection at the point of application and in the direction of the load. By assuming a deflection, the resulting P can be calculated and the energy of plate flexure determined iteratively.

A3.4 ALLOCATION OF STRAIN ENERGY AMONG THE COMPONENTS

The allocation is a trial-and-error iterative process according to the following procedure:

1. Determine the maximum load transmittable by the cylinder, cruciform and refractory concrete (that at their yield points);
2. Determine the effect of this load on the lower base mat concrete (does it cause yielding?); if it does not the process is simplified; if it does, the extent of base-mat concrete yield becomes part of the following iterative process;
3. Determine by trial and error how much yielding (displacement) by the resisting members is required to match impact energy of the pump;
4. When an approximate balance to the impact energy is achieved, the displacements and energy absorption by the components is known. Plastic yielding in compression is the major energy absorber, so the parameters affecting this component are summarized in Table A-1.

The starting point of the allocation is to determine whether or not there is sufficient strength in the components which impact the bottom liner and concrete base pad to cause plastic yielding in the base concrete. At yield,

Table A-1. Compression Parameters.

Component	Displacement at Yield (in)	Energy at Yield (in-lb)	Energy/Inch in Plastic displacement
Insulating Concrete	0.000416	0.027 per in ²	130 in-lb/in ²
Base Concrete	0.0576	130 per in ²	4500 in-lb/in ^{2*}
Cylinder at 30 Ksi yield	0.00775	6570	1.697E+06 in-lb
Cruciform at 30 Ksi yield	0.007375	3623	9.825E+05 in-lb
Cylinder at 60 Ksi yield	0.0155	13,141	3.393E+06 in-lb
Cruciform at 60 Ksi yield	0.01475	7246	1.965E+06 in-lb

From Ref. 1

the concrete displacement is shown in Table A-1 to be 0.0576 inches. At this point the displacement equation, above, for the bottom plate at $r = 18$, shows that the net load on the 3/8-in lower shell must be:

$$P = (.0576)(16\pi D)/[R^2(0.403)]$$

where 0.403 is the value of $1-x^2 + 2x^2 \ln(x)$ at $x = 0.5$, implying an R value of 36 inches. With this R value, $P = 744$ lbs, and the following displacement relation for the bottom 3/8-in steel plate applies (where the substitution, $x = r/R$ has been made).

$$\begin{aligned} w(x) &= PR^2[1-x^2+2x^2 \ln(x)]/(16\pi D) \\ &= 0.143[1-x^2+2x^2 \ln(x)], \end{aligned}$$

substituting this w value for d in Equations A-1 and A-2, the integrals for total force and energy in the concrete (assuming all elastic response) are, respectively,

$$F = E_c R^2/L \int w(x) 2\pi x dx = 2\pi E_c R^2/L(0.143) \int [1-x^2+2x^2 \ln(x)] x dx \quad (a-5)$$

and

$$J = E_c R^2/(2L) \int w^2(x) 2\pi x dx = \pi E_c R^2/L(0.143)^2 \int [1-x^2+2x^2 \ln(x)]^2 x dx \quad (a-6)$$

where E_c is concrete modulus of elasticity, 2,500,000 psi, and

$$\begin{aligned} F &= 2\pi((2,500,000)(36^2)(0.143)(.045))/32 \\ J &= \pi(2,500,000)(36^2)(0.143)^2(.01)/32 \end{aligned}$$

where (.045) and (.01) are, respectively, the closed-form evaluations of the integral $xw(x)$ and $xw^2(x)$ from 0.5 to 1, so that the total upward force in the base concrete at yield is:

$$6.283(2,500,000)(36^2)(0.143)(.045)/32 = 4.1E+06 \text{ lbs}$$

and its associated strain energy at yield is"

$$6.51E+04 \text{ in-lb}$$

The additional force required for plate flexure to support this yield (744 lbs) is negligible.

From Table A-1, considering a 36-in radius of interaction (for the refractory concrete for a total of $3.97E+05$ lbs), the total force available at yield of the cylinder, cruciform and refractory concrete is $3.08E+06$ lbs at 30 Ksi yield for steel and $5.76E+06$ at 60 Ksi yield. In other words, with the assumption of a 36-in radius of effect, the strength of the steel compression energy absorbers between the two shells is sufficient to cause yield in the base concrete at 60 Ksi yield but not at 30 Ksi.

Allocation of the strain energy among the appropriate components is done with the aid of Figure A-2. Displacement in Figure A-2 refers to total movement of the top surface of the energy absorbing components and deflection is the movement of the top surface relative to the bottom surface (so that deflection/length is strain). The total strain energy has to equal the kinetic energy of the impacting pump ($12,000/g V^2/2 = 2.74E+06$ in-lbs).

Since response is elastic for the 30 Ksi case, the force-displacement relations are linear and the displacement of the bottom concrete at the 18-in edge of the air distributor volume is:

$$0.0576(3.07E+06)/(4.1E+06) = 0.043 \text{ in.}$$

where, it is recalled, that 0.0576 is the deflection at the 18-in inner radius at concrete yield, 4.1E+06 lbs is the force required to cause plastic concrete yield, and 3.08E+06 is the force which can be supported in the cylinder cruciform and insulating concrete.

The linearity between load and deflection in the elastic realm allows the new net load on the bottom tank plate to be determined by the ratio of the total load supported and that which would be supported at yield, or $3.08E+06/4.1E+06 * 744 = 557 \text{ lbs.}$ Elastic strain energy in the bottom concrete varies as the square of the load or displacement, i.e., $[3.08E+06/4.1E+06]^2 * 6.51E+04 = 3.67E+04 \text{ in-lb.}$ The strain energy in the bottom tank shell is only 12 in-lb.

The pump kinetic energy is 2.73E+06 in-lb at impact. From Table A-1, above, it is estimated that this energy can be approximately accommodated by a plastic yield of 1 inch in the cylinder walls with the yields in other components consistent with this one for the 30 Ksi compressive yield strength in steel. Table A-2 (a duplicate of Table 3-2) shows the results of the computations using this assumption. The total is close enough to the 2.73 E+06 in-lb kinetic energy of the dropped pump that the energy allocation shown is valid. The energy in the refractory concrete is estimated as the yield load times one-half the maximum deflection (at r= 18 in). The small yield stress is not felt to justify integrating over the deflection predicted by Equation A-3.

For the 60 Ksi, the combined yield forces in the cylinder, cruciform and insulating concrete exert a force of 5.76E+06 lbs on the bottom plate and concrete, which exceeds the elastic capability of the base concrete in the annulus between the air distributor cavity and the assumed 36-in radius of interaction. The point of plastic yielding is determined by trial-and-error solution of the following equation for the y value where total upward force is 5.76E+06 lbs.

$$F_{total} = 4500\pi (y^2 - 0.5^2) * 36^2 + E_c \frac{P_y 36^4}{8LD} \int_y^1 x [1 - x^2 + 2x^2 \ln(x)] dx + P_y$$

where P_y is the net central force which makes the plate deflection by Equation A-3 equal to 0.0576 inches at the point y, the concrete yield deflection at the radial boundary between elastic and plastic yielding. This point is determined by assuming y values between r = 18 and 36 and calculating the force as determined by the above relation and P_y by Equation A-3. Figure A-3 shows the plot of the total force in the concrete as a function of y. y = 0.75 is the point of elastic yielding which produces the appropriate force balance between the bottom plate and concrete and that transmitted by the refractory concrete, cylinder and cruciform plate at their yield points. y = 0.675 is the point of elastic yielding where the force in the bottom plate and concrete equals that transmitted at yield of only the refractory concrete and the cylinder.

The strain energy which just balances the pump kinetic energy is that in the concrete when $y = .75$, plus the yield energy in the cylinder and the refractory concrete when its yield matches the point of incipient yield in the cruciform plate (note from Figure A-2 that the cruciform plate cannot yield until both the refractory concrete and the cylinder have undergone significant yielding). Energy, stress, and displacement in the concrete are shown in Figure A-4.

At 60 psi the falling pump has just sufficient kinetic energy to drive all three intervening members to the yield point and produce the maximum load and energy in the base concrete and produce significant plastic yielding in the base concrete as well as the refractory concrete and cylinder but not cause any plastic yielding in the cruciform plate because the pump kinetic energy is used up at the point where the cruciform can start to yield. It does, however impart the maximum load (yield load) in the intervening components (refractory concrete, cylinder and cruciform). This load value, $5.76E+06$ lbs is transferred to the base concrete and the appropriate y_p which sustains this load on the base concrete is 0.75. If additional kinetic energy were available it would not cause additional yielding in the base concrete because this would require a greater load and the transmitted load is already at its maximum determined by the yield of the intervening members. The additional energy would be absorbed by further yielding in the refractory concrete, the cylinder and the cruciform.

Appropriate displacements and energies for the 60-psi assumption are summarized in Table A-3 (same as Table 3-3).

Having determined y_p as 0.75, the concrete energy is calculated as the elastic component between 0.5 and y :

$$0.0576^2 E_c \pi (y^2 - 0.5^2) 36^2 / (2L),$$

plus the elastic component between y and 1:

$$E_c \left[\frac{P_y (36)^2}{16 \pi D} \right]^2 \int_y^1 \pi x [1 - 2x^2 + 2x^2 \ln(x)]^2 dx,$$

plus the plastic component (between 0.5 and y):

$$J_p = 36^2 (4500) 2\pi \int_{0.5}^y [w(x) - 0.0576] x dx.$$

where $w(x)$ is the total displacement at x determined from Equation A-3 with the P value (P_y in the relations above) which makes displacement = 0.0576 at $y = 0.75$. The results are:

1.65E+05 in-lbs for the elastic component between $x = .5$ and $.75$;

1074 in-lbs for the elastic component between $x = .75$ and 1;

1.03E+06 in-bs for the plastic component between $x = .5$ and $.75$.

Figure A-3. Limit of Plastic Yield (y) in Concrete Base.

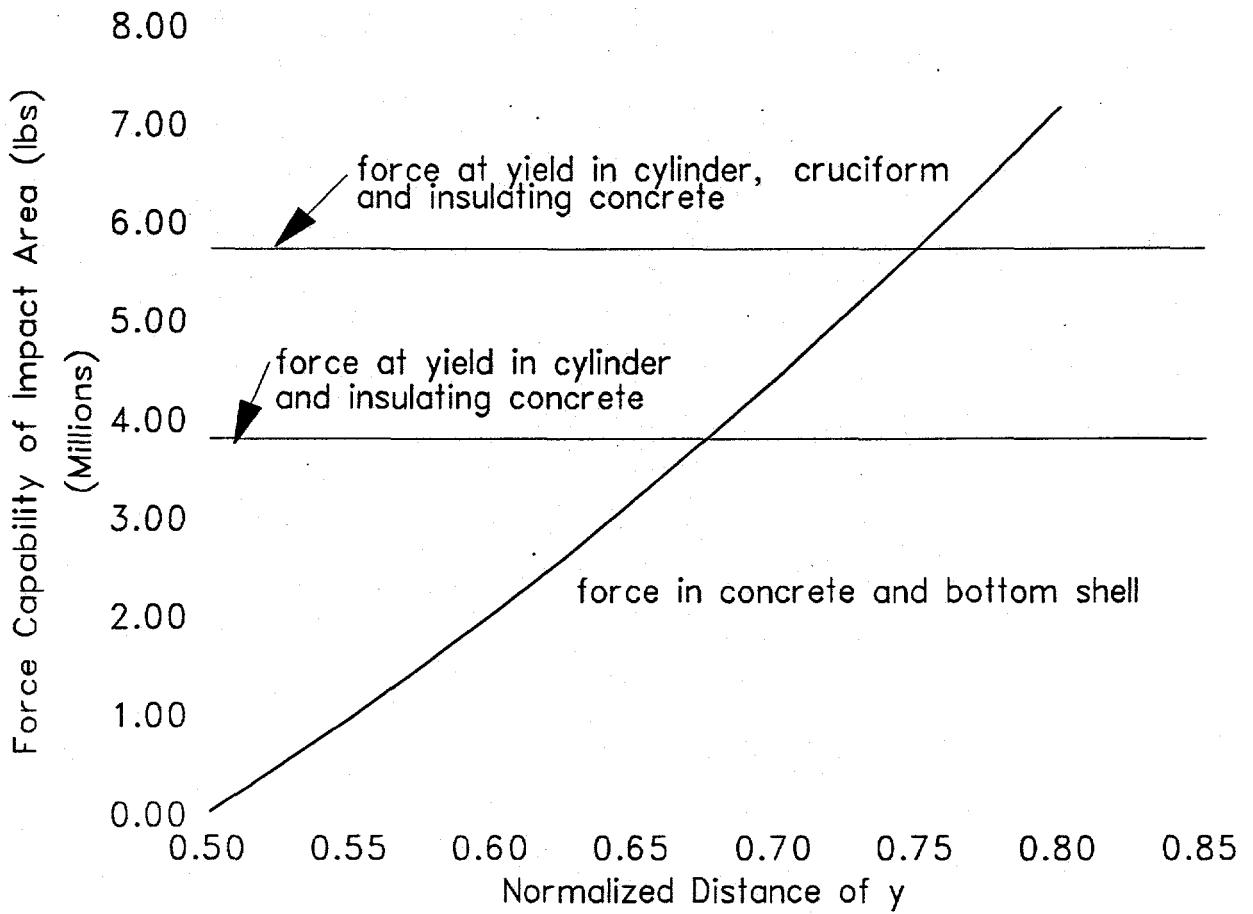
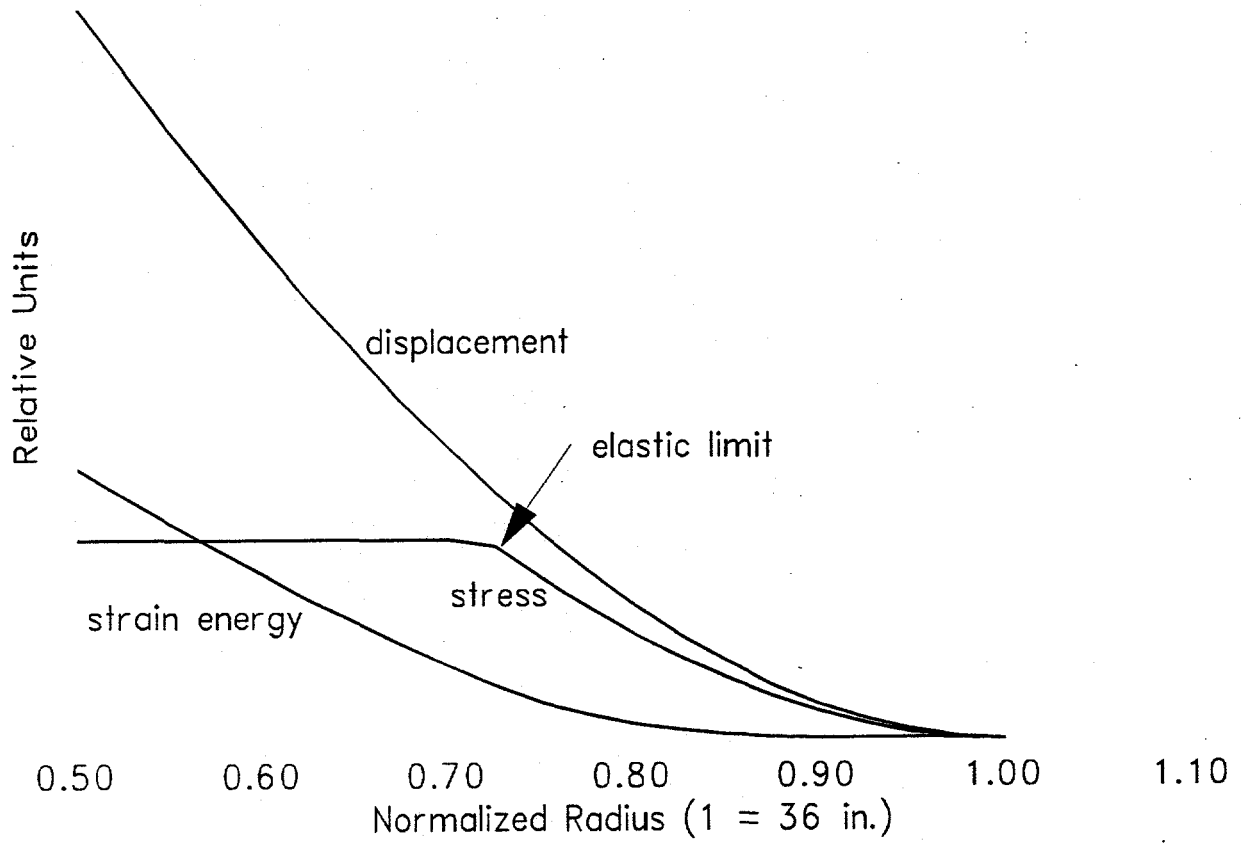


Figure A-4. Pump Impact Effect on Bottom Concrete.



These values are summarized in Table A-3 (same as Table 3-3) below. The other energy values of Table A-3 were determined with the above relations and assuming a 0.375-in deflection in the cylinder wall, with the other deflections consistent with that one as shown in Figure A-1.

Table A-2. Energy Absorption with 30 Ksi Compressive Steel Yield.

Component	Disp/Defl (in)*	Elastic Energy	Plastic Energy	Total Energy	Per Cent
Upper Shell	1.29/1.29	4.9 E04 in-lb	0	4.9E04	1.85
Refractory Concrete	1.29/1.25	neg.	2.48 E05	2.48 E05	9.34
Cylinder Wall	1.043/1.0	7271	1.7 E06	1.71 E06	64.1
Cruciform Plate	1/29/0.625	4467	6.14E 05	6.18 E05	23.3
Lower Shell	0.043	12	0	12	neg
Concrete Base Mat	0.043	36173	0	36700	1.36
Total		9.7 E04	2.56 E06	2.66 E06	100

Table A-3. Energy Absorption with 60 Ksi Compressive Steel Yield.

Component	Disp/Defl (in)	Elastic Energy	Plastic Energy	Total Energy	Per Cent
Upper Shell	.829/.829	2.61 E04 in-lb	0	2.61 E04	0.98
Refractory Concrete	.829/.625 (av)	neg.	1.25 E05	1.25 E05	4.7
Cylinder Wall	0.79/0.375	2.9 E04	1.27 E06	1.3 E06	49
Cruciform Plate	0.625/neg.	1.8 E04	0	1.8 E04	0.67
Lower Shell	0.204	1318	0	1318	0.05
Concrete Base Mat	0.204	1.66 E05	1.03E06	1.2E06	45
Total	0.829	2.4 E05	2.37 E06	2.67 E06	100

* Displacement and deflection: total movement of top surface, and movement relative to bottom surface, respectively.

The assumption of a higher yield stress in the steel compression components between the upper and lower plates causes yielding in the base concrete, as expected, but not enough to compromise the overall resistance of the tank bottom to a leak induced by a dropping mixing pump. For a given deflection the induced elastic energy in the bottom plates is independent of the assumed radius of interaction with the plate because it is proportional to P^2R^4 and P is proportional to $1/R^2$ for a given deflection. It affects the base concrete, however, because yield strength in the cylinder wall and cruciform may be sufficient to drive it to the yield point. If the stress in the concrete stays in the elastic realm the energy actually decreases as the assumed area of interaction increases because the induced stress, S , is inversely proportional to area, A , and total energy is proportional to $S^2A \propto 1/A$. When yielding occurs, the energy also decreases with increasing radius of interaction, but not as rapidly as with purely elastic response.

The choice of area of interaction with the bottom is not a significant parameter in calculating energy absorption, because the energy contribution of the area-dependent components (bottom plates and base concrete--which are also the leak barriers) is nearly independent of the choice of area and not large enough to cause significant leakage.

It is advisable to examine the effects if only a small region surrounding the air distributor cavity is affected. Therefore, it is worth examining a "worst-case" scenario, which is treated in the following paragraphs. The flexural energy in the lower plate is so low, it doesn't matter what the materials response assumptions are regarding this component. For the upper shell (the 1/2-in shell), however, the yield strength in the cylinder wall and the cruciform plate determine how much deflection, and thereby, how much energy is imparted to it.

The worst case is assumed to be where all welds break by brittle fracture and negligible energy is absorbed in the process. The 48-in, 1-in thick plate is driven down onto the cylinder between the plates and it is forced onto the concrete at the edge of the air distributor cavity. The drawing of Figure 1-2 indicates the inside of the cylinder wall is at the inside of the air distributor cavity. Therefore, a 1/2-in ring around this cavity crushed. Since concrete yield is low, this ring region and the refractory concrete in the ring region between the cylinder wall and the outer diameter of the 1-in plate (a 6-in radius ring region) are the only effective energy absorption regions. The refractory concrete will be crushed and the base concrete will be crushed, also, and will be chipped or flaked off into the air distributor cavity.

These absorb energy at a rate per inch of:

$$130\pi(24^2 - 18^2) + 4500\pi(18.5^2 - 18^2) = 185,087 \text{ in-lbs}$$

which ignores their shear strength. Upper limit displacement (before the 1-in plate strikes the lower shell and concrete) is 8 inches. Therefore, $8(185,087) = 1.48E+06$ in-lbs, which is 54% of the energy of the impacting pump has been dissipated. The full energy of the impacting pump could not penetrate this concrete or the lower plate, with this radius of interaction as shown in Section 3. Therefore, there is no concrete leak because of this and the net effect is that a portion of the concrete of the air distributor cavity will flake off into the cavity and a 6-in wide ring of the refractory concrete

will be crushed. Of course, both tank walls will leak because of the assumption of the broken welds, but the leak will be retained by the concrete base.

Any severe damage to the concrete from the impacting pump, because of its central location, could cause cracking and spalling at the top of the air distributor cavity. This local damage will help absorb the shock and energy of the impacting pump and prevent damage through the total thickness where a leak path could be developed.

This page intentionally left blank.

Appendix B

**DETAILS OF MISSILE STRIKE AND
PENETRATION CALCULATIONS**

This page intentionally left blank.

APPENDIX B

The following appendix is excerpted and slightly modified from REF. 15 which was a study on tornado missile penetration of concrete and metal containers for waste storage at Savannah River. The descriptions apply for this study.

This page intentionally left blank.

DETAILS OF MISSILE STRIKE AND PENETRATION CALCULATIONS

This appendix contains calculational and other details in support of the main body of the report.

B1.0 MISSILE PENETRATION (PERFORATION) OF CONCRETE

This study used a formula for concrete penetration which was derived on the basis of tests performed by the Commissariat a l'Energie Atomique - Electricite de France (CEA-EDF) (9). Electric Power Research Institute, Palo Alto, CA (EPRI) recommends this formula as providing the best match to experimental data over a full range of missile velocities.

Its form is:

$$T_p = 0.765\sigma_c^{-3/8}(W/D)^{1/2}V_i^{3/4} \quad (B1-2)$$

where

T_p = thickness of wall that is penetrated 50% of the time for the given missile (in)

σ_c = concrete compression strength (psi)

W = missile weight (lb)

D = effective diameter (in)

$D = 2 [A/\pi]^{.5}$ where A represents an effective impact area

V_i = incident velocity (ft/sec)

The combination of impact area and velocity obviously governs barrier penetration for a given missile.

In this study, it is assumed that only one interaction with the target is possible, and there is no interest in missile ricochet conditions or velocity after penetration, as there is with certain other studies.

B2.0 MISSILE PENETRATION (PERFORATION) OF STEEL BARRIERS

The Hagg-Sankey (8) method is utilized for interactions with steel walls on the basis of EPRI recommendations (9). This method predicts steel wall perforation as a "two-phase" process. In the first phase, resistance is affected only by local shear and compression. In the second phase, the wall has had time to "stretch" in the plane of the wall, with tensile resistance also contributing. Perforation can occur in either phase. It is considered

the only method available which realistically predicts effects when tensile stress is the most important contributor to perforation resistance. Figure B2-1 illustrates the process. In the figure, M_1 is the missile mass, m_{21} is the mass of the sheared punching which is ejected along with the missile if stage 1 failure occurs, m_{22} is the mass between the two plastic hinges, and m_3 is the portion (a fraction of m_{22}) which is effectively accelerated along with m_{21} . The fraction is determined as the square of the ratio of the radius of gyration of m_{22} to length of plastic hinge and is 0.34 for a plastic hinge of length $3T$. The equations involved are described below. The Hagg-Sankey formalism requires initially that M_2 , the barrier mass which can be effectively accelerated along with the missile, $m_{21} + m_3$, be calculated. Its value is:

$$M_2 = \rho[A + 1.36 \Phi(V_{ni})T A]T \quad (B2-1)$$

where

- ρ = density of steel (slugs/ft³)
- A = effective impact area of missile (ft²)
- T = barrier thickness (ft)
- V_{ni} = impact velocity component normal to barrier (fps)

$\Phi(V_{ni})$ is a function of impact velocity normal to the barrier which accounts for the distance in the wall from point of missile contact that is affected by the impact. From a private communication with Sankey, co-author of the method, the following empirical relation has been derived:

$$\Phi(V_{ni}) = \frac{2}{1 - e^{-0.00138V_{ni}}} \quad (B2-2)$$

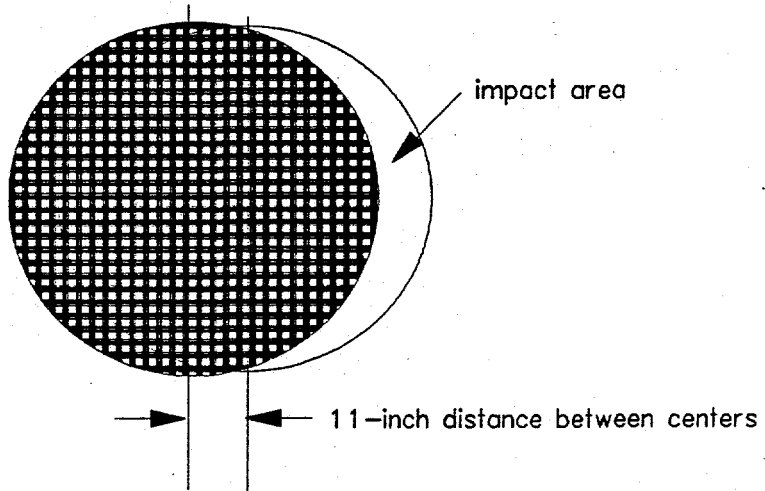
which fits the measured results of Westinghouse (10) for missile penetration of their turbine housing (which requires that $\Phi(V_{ni}) = 2$ at 4000 fps, 3 at 800 fps, and 10 at 100 fps).

Also needed is the initial missile energy loss, E_1 , required to accommodate momentum conservation as M_2 is accelerated.

$$\Delta E_1 = 0.5M_1V_{ni}^2 \left[1 - \frac{1}{M_1 + M_2} \right]$$

where M_1 is missile mass.

Figure B2-1. Missile Interaction with Steel Walls and Hagg-Sankey Parameters.



In order for Phase I failure to occur, E_1 must exceed the effective strength of the barrier in local compression and shear ($E_c + E_s$).

$$E_c = AT\xi_d \quad (B2-4)$$

$$E_s = K\tau_d PT^2 \quad (B2-5)$$

where

ξ = an effective compressive strain (0.07)

σ_d = compressive yield strength (-50,000 psi)

K = constant accounting for the amount of shear energy used (0.45)

τ_d = the shear yield strength of the barrier ($\approx 30,000$ psi)(8)

P = the periphery of the missile impact area.

Note that 50,000 and 30,000 are the static yield stresses for compression and shear, which is a conservative assumption. Use of the higher dynamic yield stresses would predict a smaller number of penetrations.

Figure B2-2 shows how Equation B2-5 is derived. It is simply the yield stress in compression times area of application times displacement (ξTA). The elastic component is small compared to the plastic deformation and is ignored, as is the elastic energy in the missile itself. The strength alloy of the missiles is assumed sufficient to prevent its yielding, and its elastic energy storage is even less than that in the wall. Such an assumption is very conservative for tornado missiles since they typically absorb much of the energy of the interaction. Figure B2-3 shows how the shear strain energy term (Equation B2-6) is derived. The original Hagg-Sankey work listed Equation B2-7 without explanation other than that K was determined experimentally to be in the range from 0.3 to 0.5. Shear strain energy (in the plastic flow regime) is $\tau_d \lambda PT$, where λ is the length of the plastic hinge, PT is the area over which the shear stress is manifest, and ϕ is the angle of deformation (i.e., that of permanent set, since it has been assumed that the elastic contribution is negligible).

For a plastic hinge length of between 2T and 3T, and a shear yield stress of 30,000 psi, the deformation angle would be in the range from 0.2 to 0.5 radians. This value is reasonable and is consistent with Hagg-Sankey experiments. Inserting appropriate constants and converting to ft-lb units we have:

$$E_c = 292 AT \text{ ft-in}$$

$$E_s = 4500AT_2 \text{ ft-in} \quad (B2-6)$$

Figure B2-2. Compressive Energy in Wall (E_c).

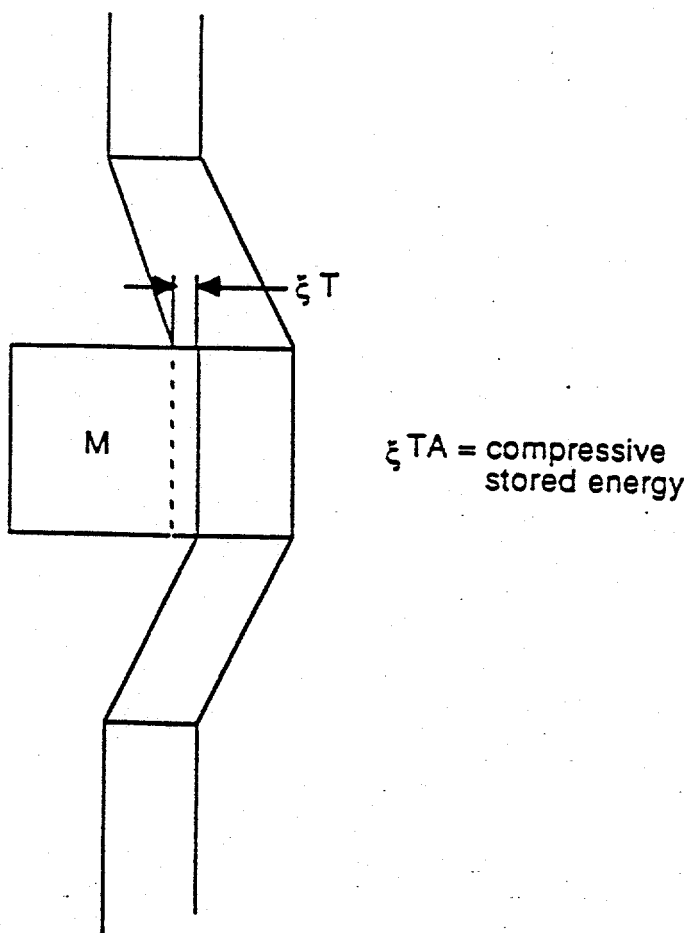
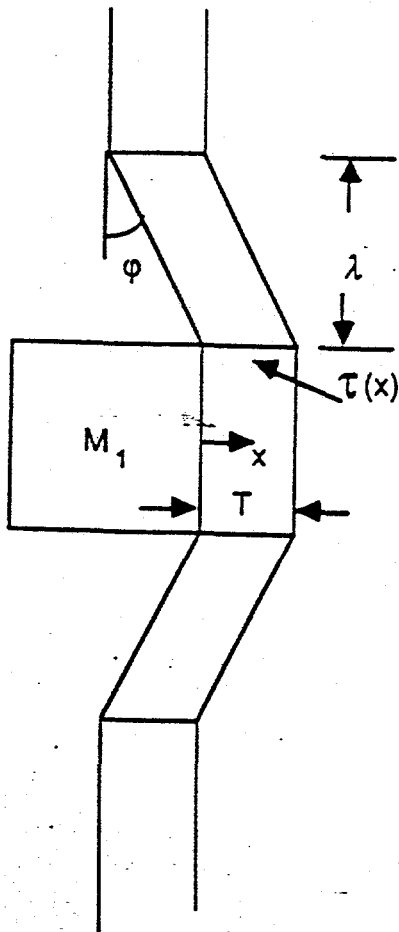


Figure B2-3. Shear Energy Associated with Missile Impact.



P = periphery of punched-out (sheared) section.

λ = length of plastic hinge

ϕ = angle of deformation caused by plastic shear

$$\tau(x) = \left(\frac{T-x}{T} \right) \tau_d$$

where τ_d = elastic limit in shear (psi)

Work of shear deformation (E_s)

$$= \lambda \phi P T \frac{\tau_d}{T} \int_0^T (T-x) dx$$

$$= K P T^2 \tau_d, \text{ where } K = \frac{\lambda \phi}{2T}$$

If E_1 exceeds $E_c + E_s$, the barrier fails during the so-called Phase I and the missile has a residual normal velocity, V_{ne} given by:

$$V_{ne} = \frac{M_1 V_{ni}}{M_1 + M_2} + \sqrt{\left[\frac{M_1 V_{ni}}{M_1 + M_2} \right]^2 - \frac{2(E_c + E_s) m_3 - M_1 V_{ni}^2 (m_3 - m_1)}{(M_1 + M_2)(M_1 + m_2)}} \quad (B2-7)$$

where

m_2 = the mass of the target wall having the same cross sectional area as the missile

$$m_3 = M_2 - m_2$$

Equation B2-7 has been derived from the equations of energy conservation:

$$1/2 M_1 V_1^2 - 1/2 (M_1 + M_2) V_{ne}^2 - 1/2 M_3 V_3^2 - E_s - E_c = 0$$

and momentum conservation:

$$M_1 V_1 - (M_1 + m_2) V_{ne} - m_3 V_3 = 0$$

If $E_c + E_s$ exceeds ΔE_1 , the tensile-strength phase (or Phase II) or the interaction ensues, and then E_2 , the kinetic energy of the moving wall and missile which must be resisted by tensile strength in the target wall, is determined.

The relations are:

$$E_2 = 1/2 M_1 V_{ni}^2 \left(\frac{M}{M_1 + M_2} \right) \quad (B2-8)$$

$$E_T = Q \xi_T \sigma_d \quad (B2-9)$$

where

Q = the effective volume which can be stressed in tension (assumed to be approximately equal to the volume associated with $m_{21} + m_{22}$ of Figure B2-1)

ξ_T = the effective tensile strain (0.05)

σ_d = the tensile ultimate strength (same as compression) in steel

with appropriate constants,

$$E_T = \frac{208(m_{22} + m_{21})}{\rho_{steel}} = 208(3PT^2 + AT)$$

If E_1 exceeds E_2 , the breach of the target wall is prevented. If not, the missile breaches the target wall and exits with a determinable velocity (which is of no interest to this study).

In the Phase 2 portion of steel penetration described above, the Hagg-Sankey formula has been modified somewhat to accommodate wall thicknesses which are much less than those for which the formula was developed. The original Hagg-Sankey formulation was based on experiments with models of turbine missiles exiting through turbine casing walls which are relatively thick. The appropriate distance beyond the boundaries of the penetrating missile over which tensile stresses were considered to be effective was empirically determined and was typically a few inches in length (three times the wall thickness). If the same relation were used for the 3/8-in or 1/2-in tank wall, less than 2 inches would be effective. Such a short range is unrealistically low.

A better measure of the effective length of tensile effect should be the distance traveled by an acoustic wave during the time of interaction of the missile with the wall. Acoustic velocity in steel $(b/\rho)^{0.5}$ where b is bulk modulus in psi and ρ = density in slugs per cubic inch) approaches 200,000 in/s, and the velocity of the pump missile is 35 fps or roughly 400 ips. If it is assumed that 1/2-in deflection of the tank wall occurs before significant wall effects are manifest, then the acoustic wave can travel many feet in the metal during this time. This has justified an adjustment of the parameter to make it approach the values of the other two empiricisms compared (Hagg-Sankey is the most conservative of these algorithms).

It is compared to other empiricisms for calculating steel wall perforation (the Stanford Research Institute [SRI] and Ballistic Research Laboratory [BRL] formulas--see Reference 11) for each steel wall penetration calculation. Comparison penetration velocities calculated for each of the three methods are shown in Table 3-2. Conservative materials properties have been used in these formulas. 50,000 psi is the tensile ultimate used for steel (which is rather low and augments the conservatism of the calculated penetration probabilities). Conservative assumptions and comparisons with other formulas are used in lieu of experimental data on wall perforation for the walls of this type.